

# Efficiency Optimization of PMSM Based Drive System

Waleed Hassan and Bingsen Wang  
Department of Electrical and Computer Engineering  
Michigan State University  
2120 Engineering Building  
East Lansing, MI 48824  
Emails: hassanwa@msu.edu; bingsen@egr.msu.edu

**Abstract**—The proposed work in this paper is a combination of analytical and numerical methods that are able to calculate the harmonic losses of permanent magnet synchronous machine (PMSM) at any operating point with less execution time and adequate accuracy. Both the fundamental and harmonic losses of the machine in conjunction with the inverter losses are modeled such that the inverter-motor efficiency can be tested for different conditions. Numerical simulation of the field oriented control have been conducted and results include current, modulation index, power factor, switching frequency and all the variables in the drive system. Furthermore, Maximum efficiency control strategy has been chosen such that the drive system can work at the most efficient condition at all operation points. The proposed work is presented in the context of drive system that is based permanent magnet synchronous machine (PMSM). However, the proposed method can be extended to induction motor drive system or any motor use PWM in control of the inverter output voltage.

## I. INTRODUCTION

Loss modeling and control of high performance motor drive system has attracted significant research attention [1]–[4]. The reduced system losses not only can be translated to higher efficiency and lowered operating cost, but also can reduce the thermal stress on various components or sub-systems and in return will improve the reliability of overall system. The reduction of life-cycle cost due to the improved reliability is of great practical significance in many of the cost-sensitive applications of the electric drive systems.

The efficiency and power density of permanent magnet synchronous machines (PMSMs) have been studied by several authors [2], [4]–[6]. It has been shown that PMSM can achieve significantly higher efficiencies than induction motors when used in adjustable speed drives. Analytical method for estimating the fundamental losses of surface mounted PMSM has been proposed in [5]. Several researchers have utilized electrical model of PMSM that includes a parallel resistance that accounts for core losses in high performance applications [2], [4]. It can be concluded that both copper and core losses need to be accounted for in the analysis and control of high performance motor drives. The core losses are due to both the fundamental and harmonics excitations.

The existing optimization methods of the drive system is focused on the fundamental losses of electric machines. The inverter losses are often not counted in the optimization

process although the modeling of inverter losses is already known [7]. A study on the harmonics losses of transformers has been reported [8]. This paper proposes an integrative approach to optimize the efficiency of the drive that including the fundamental losses and the losses due to the switching of the inverter.

The rest of the paper is organized as the following. Section II provides analytical model of PMSM harmonic losses based on the armature reaction field produced by three-phase current of stator winding. Double Fourier series for naturally sampled sinusoidal PWM (SPWM) has been utilized for evaluation and analysis. Section III presents analytical-numerical method of loss calculation for three-phase inverter controlled by SPWM. The optimal-efficiency control strategy is implemented in section IV. The results and conclusion are presented in section V.

## II. HARMONICS LOSS MODELING OF PMSM

The core losses in the machine consist of two components, i.e., hysteresis and eddy current losses. Both types of core loss are due to time variation of the flux density in the core. The complete expression for core losses in  $[\text{W m}^{-3}]$  is:

$$P_{cd} = K_e \sum_{n=1}^{\infty} (n\omega_s)^2 B_{p,n}^2 + K_h \sum_{n=1}^{\infty} n\omega_s B_{p,n}^{\beta} \quad (1)$$

where  $K_e$  is the eddy loss coefficient;  $K_h$  is the hysteresis loss coefficient;  $B_{p,n}$  is the peak flux density of the  $n$ th-order; and  $\omega_s$  is fundamental angular frequency of applied voltage [9].

### A. Harmonic Flux Density

In this section analytical model for surface mounted PMSM motor harmonic loss is developed based on the work published in where the armature reaction field produced by the stator winding is predicted. The armature reaction field produced by a three-phase stator winding is:

$$B_{3\phi}(\alpha, r, t) = B_p \sin(n\omega_r t + v\alpha + \theta_n) \quad (2)$$

where  $\omega_r = P_p \omega_m$  is the electrical rotor angular speed in  $[\text{rad s}^{-1}]$ ; the amplitude of flux density  $B_p$  due to the  $n$ th-

order armature reaction current is determined by:

$$B_{p,n} = \mu_0 \frac{2W}{\pi\delta} \sum_n I_n \sum_v \frac{1}{v} K_{sov} K_{dpv} F_v(r) \quad (3)$$

### B. Eddy Current Loss

Once the maximum amplitude of the flux density has been determined, which results from the armature space vector current, the procedure of finding accurate model for core loss is shown in the following approximate expression.

$$P_{ed} = K_e \sum_n (n\omega_r)^2 B_{p,n}^2 \quad (4)$$

Substituting (3) into (4) and defining the volume in which the loss is evaluated, the expression for eddy core loss as will be reached as

$$P_e = K_{em} \sum_{n=1}^{\infty} (n\omega_r)^2 I_n^2 \quad (5)$$

where  $\rho_i$  is the mass density of the steel core material in [kg m<sup>-3</sup>];  $V$  is the steel core volume in [m<sup>3</sup>]; and their product gives the weight of the core material in [kg].  $K_{em}$  is defined as:

$$K_{em} = (\rho_i V) K_e \left( \mu_0 \frac{2W}{\pi\delta} \right)^2 \left( \sum_v \frac{1}{v} K_{sov} K_{dpv} F_v(r) \right)^2$$

### C. Hysteresis Loss

Following the same procedure as the last section, an expression for hysteresis loss can be reached as presented in (6).

$$P_h = K_{hm} \sum_{n=1}^{\infty} n\omega_r I_n^2 \quad (6)$$

where  $K_{hm}$  is defined as:

$$K_{hm} = (\rho_i V) K_h \left( \mu_0 \frac{2W}{\pi\delta} \right)^2 \left( \sum_v \frac{1}{v} K_{sov} K_{dpv} F_v(r) \right)^2$$

The final expression for the core loss in [W] is given by:

$$P_c = P_e + P_h = K_{em} \sum_{n=1}^{\infty} (n\omega_r)^2 I_n^2 + K_{hm} \sum_{n=1}^{\infty} n\omega_r I_n^2 \quad (7)$$

Close examination of  $K_{em}$  and  $K_{hm}$  shows that they are constant for a given machine design since they solely depend on the machine dimensions.

### D. SPWM Harmonics Analysis

If the losses associated with fundamental is excluded from (7), the core harmonic loss can be expressed as:

$$\begin{aligned} P_{c,h} &= P_{e,h} + P_{h,h} \\ &= K_{em} \sum_{n=2}^{\infty} (n\omega_r)^2 I_n^2 + K_{hm} \sum_{n=2}^{\infty} n\omega_r I_n^2 \end{aligned} \quad (8)$$

It is clear that the motor harmonics loss can be fully evaluated if the amplitudes of current harmonics determined.

For three-phase inverter with two-level phase legs, a balanced set of three-phase line-line output voltages is obtained

if the references are displaced by 120°. Under these conditions, the line to line voltages are given for naturally sampled PWM by [10]

$$\begin{aligned} v_{ll} &= \frac{\sqrt{3}V_{dc}}{2} M \cos(\omega_o t + \pi/6) \\ &+ \frac{4V_{dc}}{\pi} \sum_{m=1}^{+\infty} \sum_{\substack{n=-\infty \\ n \neq 0}}^{+\infty} \left[ \frac{J_n\left(\frac{m\pi}{2}M\right)}{m} \sin\left(\frac{(m+n)\pi}{2}\right) \sin\left(\frac{n\pi}{3}\right) \right. \\ &\quad \left. \times \cos(m\omega_c t + n(\omega_o t - \pi/3)) \right] \end{aligned} \quad (9)$$

The major significant side-band harmonics are at the frequency of  $f_h = f_s \pm 2f_o, f_s \pm 4f_o, 2f_s \pm 5f_o$ .

The surface mounted PMSM can be analyzed as a single phase circuit that consists of series impedance and back emf since the reactances on the d-axis and the q-axis are identical. At harmonic frequencies 3,6,9 stator resistance and back emf are neglected so that the motor modeled as synchronous inductance only. The motor phase current can be determined by the phase voltage and the synchronous inductance of the stator winding. With the assumption of star connection of PMSM, the phase current is given by:

$$I = \frac{v_{ll}/\sqrt{3}}{\omega L_s} \quad (10)$$

Plugging equation (9) in equation(10) yields the harmonics of the stator current. Once the stator harmonic current is determined, the harmonic losses are readily to be calculated.

## III. LOSS OF VOLTAGE SOURCE INVERTER

The majority of harmonic losses of the motor, which is caused by PWM carrier frequency, can be minimized by increasing the inverter switching frequency. Nonetheless, the inverter switching loss will concurrently increase, as detailed in the subsequent section. Therefore, for achieving global optimization of the system, one needs to define the value of the optimal frequency that minimizes the motor harmonic loss and inverter losses together. The aim of this section is to provide analytical model for the calculation of power losses in IGBT-based voltage source inverter used in PMSM drive system. The inverter parameters of the semiconductor switches in the inverter have been extracted from the data sheets of FAIRCHILD, RURG5060 and HTGT30N60A4 modules.

A number of different methods have been proposed to estimate the losses of voltage source inverters. The first is based on the complete numerical simulation of the circuit by specific simulation programs with integrated or parallel-running losses calculations. The second is to calculate the electrical behaviour of the circuit based on analytical behaviour model [7]. For accurate estimation of the losses during the transient time and all operating conditions, a hybrid model has been developed. In this model, the operating conditions that are resulted from the numerical simulation of the motor drive system are utilized in the analytical model. The losses in a power-switching device consist of conduction losses, switching losses and off-state blocking loss.

### A. Switching Losses of VSI

The equation for the switching loss  $P_{ls}$  of a VSI with sinusoidal ac line current and with IGBT switching devices is given by:

$$P_{ls} = \frac{6}{\pi} \cdot f_s \cdot (E_{on,I} + E_{off,I} + E_{off,D}) \cdot \frac{V_{dc}}{V_r} \cdot \frac{I_L}{I_r} \quad (11)$$

where  $f_s$  is the VSI switching frequency;  $V_{dc}$  is the dc link voltage;  $I_L$  is the peak value of the ac line current that is assumed sinusoidal;  $E_{on,I}$  and  $E_{off,I}$  are the turn-on and turn-off energies of the IGBT, respectively;  $E_{off,D}$  is the turn-off energy of the power diode due to reverse recovery current.

### B. Conduction Losses of VSI

In contrast to the switching losses, the conduction losses are directly depending on the modulation function. For the carrier based PWM method, the conduction losses of the IGBT and the diode can be expressed as:

$$P_{lc,I} = \frac{V_{CE,0}}{2\pi} \cdot I_L \left( 1 + \frac{M \cdot \pi}{4} \cdot \cos(\phi) \right) + \frac{r_{CE,0}}{2\pi} \cdot \left( \frac{\pi}{4} + M \left( \frac{2}{3} \cdot \cos(\phi) \right) \right) \quad (12)$$

$$P_{lc,D} = \frac{V_{F,0}}{2\pi} \cdot I_L \left( 1 - \frac{M \cdot \pi}{4} \cdot \cos(\phi) \right) + \frac{r_{CE,0}}{2\pi} \cdot \left( \frac{\pi}{4} - M \left( \frac{2}{3} \cdot \cos(\phi) \right) \right) \quad (13)$$

where  $M$  is the modulation index and  $\phi$  is the displacement angle between the fundamental of modulation function and the load current. The total inverter losses at different operation points will be analyzed in the next subsection.

### C. Total Losses of VSI

The total losses of the VSI have been evaluated based on the parameters that are listed in Table I.

TABLE I  
PARAMETERS OF THE SEMICONDUCTOR DEVICES OF THE VSI.

Power Devices	Parameters			
IGBT	$I_{ref}$ (A)	50	$V_{ref}$ (V)	600
	$E_{on,I}$ (mJ)	0.6	$E_{off,I}$ (mJ)	0.966
	$V_{CE,0}$ (V)	1.6	$r_{CE,0}$ (mΩ)	15
Diode	$r_{F,0}$ (mΩ)	8	$V_{F,0}$ (V)	1.6
	$E_{off,D}$ (mJ)	0.7		

A plot of the switching loss for a range of switching frequencies is shown in Fig. 1. It is clear that the switching loss is proportional to switching frequency and maintains constant for a given load current and switching frequency. The conduction loss depends on load displacement angle, modulation index and load current. Fig. 2 illustrates the variations of the conduction losses with the load displacement angle under different loading conditions. The plot of conduction loss equation shows that the loss is maximized when the displacement angle is zero and decreases as the displacement angle increases or decreases from zero. In field oriented control of variable speed drive

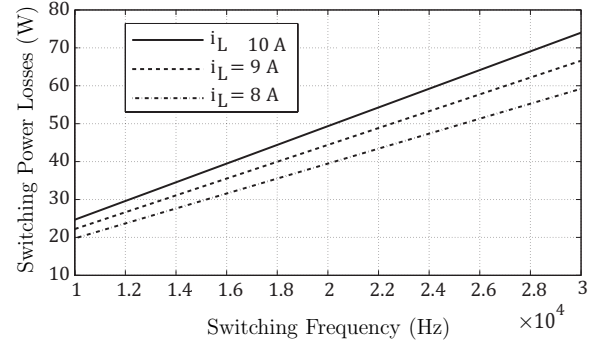


Fig. 1. Switching losses of VSI at different load currents.

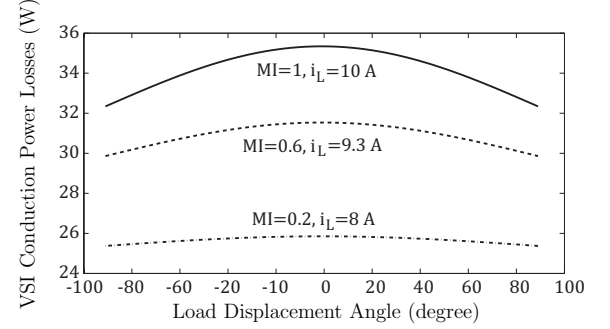


Fig. 2. Switching losses of VSI at different modulation indices.

system, for a given speed command the controller will assign voltage proportional to that speed by means of modulation action. However, increasing the motor speed requires higher line to line voltage and causes the motor to draw higher current for constant load torque. In other words, increasing the motor speed will increase the inverter losses since the current and modulation index will be higher.

## IV. LOSS MINIMIZATION CONTROL STRATEGY

The combined copper losses and iron fundamental losses are minimized through control strategy developed in [4]. The controllable losses can be minimized by proper choice of the armature current vector. It is a common practice to set the current  $i_d = 0$ . As a result, the armature current vector that is in phase with the back EMF is applied. In addition, irreversible demagnetization of permanent magnets can be avoided. The recent development of the permanent magnets has brought materials with high coercivity and high residual magnetism. Therefore, several control methods have been proposed to improve the performance of the PM motor drives. In such control methods, the d-axis component of armature current is actively controlled according to the operating speed and load conditions. In the next subsection, the basic equations of motor model needed to develop the control algorithm are presented.

### A. Modeling Fundamental Losses of PMSM

The steady state  $d, q$  model of PMSM is shown in Fig. 3. The fundamental iron loss consists of hysteresis loss and eddy current loss. Herein, these two loss components are lumped

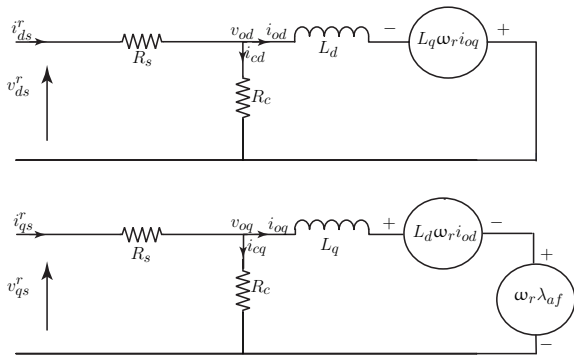


Fig. 3. Steady state equivalent circuit of PMSM including core loss resistance.

into a single quantity, which is represented by the core loss resistance  $R_c$ . As shown in Fig. 3, the voltage equations of PMSM in steady-state are expressed as:

$$\begin{aligned} \begin{bmatrix} v_{rs}^{ds} \\ v_{qs}^r \end{bmatrix} &= R_s \begin{bmatrix} I_{od} \\ I_{oq} \end{bmatrix} + \frac{R_c + R_s}{R_c} \begin{bmatrix} v_{od} \\ v_{oq} \end{bmatrix} \\ \begin{bmatrix} v_{od} \\ v_{oq} \end{bmatrix} &= \begin{bmatrix} 0 & -L_q \omega_r \\ L_d \omega_r & 0 \end{bmatrix} \begin{bmatrix} I_{od} \\ I_{oq} \end{bmatrix} + \begin{bmatrix} 0 \\ \lambda_{af} \end{bmatrix} \end{aligned} \quad (14)$$

where

$$\begin{aligned} I_{od} &= I_{ds}^r - I_{cd}; & I_{oq} &= I_{qs}^r - I_{cq} \\ I_{cd} &= -\left(\frac{L_q}{R_c}\right)\omega_r I_{oq}; & I_{cq} &= \frac{1}{R_c}(\lambda_{af} + L_d I_{od})\omega_r \end{aligned} \quad (15)$$

The armature current  $i_a$ , the terminal voltage  $v_a$  and the torque  $T_e$  are expressed as:

$$i_a = \sqrt{i_d^2 + i_q^2}; \quad v_a = \sqrt{v_d^2 + v_q^2} \quad (16)$$

$$\begin{aligned} v_a &= \sqrt{(R_s i_d - \omega_r L_q i_{oq})^2 + (R_s i_q + \omega_r (\lambda_{af} + L_d i_{od}))^2} \\ T_E &= \frac{3}{2} \frac{P}{2} [\lambda_{af} I_{oq} + (L_d - L_q) I_{od} I_{oq}] \end{aligned} \quad (17)$$

The copper loss  $P_{Cu}$  and the iron loss  $P_{Fe}$  are determined by:

$$\begin{aligned} P_{Cu} &= \frac{3}{2} R_s \left[ \left( i_{od} - \frac{\imath L_q i_{oq}}{R_c} \right)^2 + \left( i_{oq} + \frac{\imath (\lambda_{af} + L_d i_{od})}{R_c} \right)^2 \right] \\ P_{Fe} &= \frac{3}{2} \frac{\omega_r^2}{R_c} [(L_q i_{oq})^2 + (\lambda_{af} + L_d i_{od})^2] \end{aligned} \quad (18)$$

### B. Condition for Minimized Losses

The total electric power loss  $P_E = P_{Cu} + P_{Fe}$  can be expressed as a function of  $i_{od}$ ,  $T_e$  and  $\omega_r$ . Under the steady state, the electrical loss  $P_E$  is function of  $i_{od}$ . Nevertheless, for surface mounted PMSM  $L_d = L_q$ . Hence, simple expression for  $P_E$  can yield. By differentiation of  $P_E$  with respect to  $i_{od}$ ,

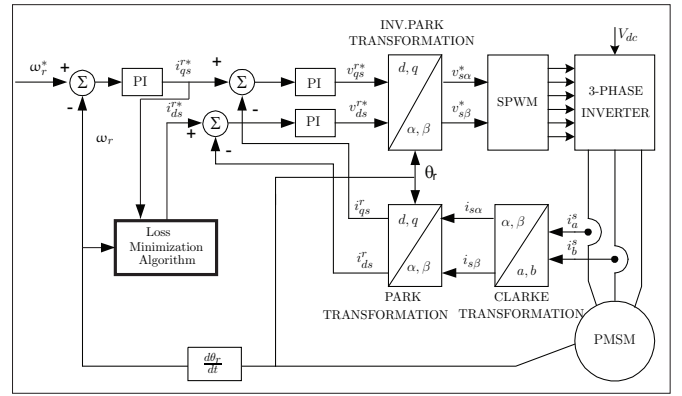


Fig. 4. Field oriented control diagram including loss minimization algorithm.

the condition for  $i_{od}$  that minimizes the controllable losses results has been found.

$$I_{od} = -\frac{\lambda_{af}(R_s + R_c)\omega_r^2 L_d}{R_s R_c^2 + \omega_r^2 L_d^2 (R_s + R_c)} \quad (19)$$

The role of the loss minimization algorithm in the field oriented control system is shown in Fig. 4. The simulation results will be presented in the next section.

## V. SIMULATION RESULTS AND DISCUSSION

The machine parameters of surface mounted PMSM that have been used in the simulation are listed in Table II. The field oriented control system includes the loss minimization algorithm implemented in MATLAB/SIMULINK. The Motor harmonic losses of the machine are calculated by MATLAB block using the variables that is obtained from SIMULINK for various operation conditions. The converter losses are directly calculated by use of SIMULINK system with parameters that are generated by FOC subsystem. The results and discussion are presented in three subsections; FOC under loss minimization control strategy (LMCS), VSI-motor fundamental losses, and VSI-motor harmonic losses.

TABLE II  
MACHINE PARAMETERS.

Parameter	Value	Units
Number of pole pairs	4	
Stator resistance	0.52	$\Omega$
Core loss resistance	450	$\Omega$
Rated speed	4500	rpm
Rated torque	6	Nm
Rotor flux linkages	0.08627	Wb
Rated peak voltage per phase	150	V
Rotor inertia $J_m$	0.00036179	kgm <sup>2</sup>
Viscous friction coefficient $B_m$	$9.444 \times 10^{-5}$	Nms
$L_d$	0.0013	H
$L_q$	0.0013	H

### A. FOC with Loss Minimization Control

The dynamic responses of currents, speed and torque at rated conditions are shown in Fig. 5 and Fig. 6, respectively. The system reaches the steady state with smooth dynamic

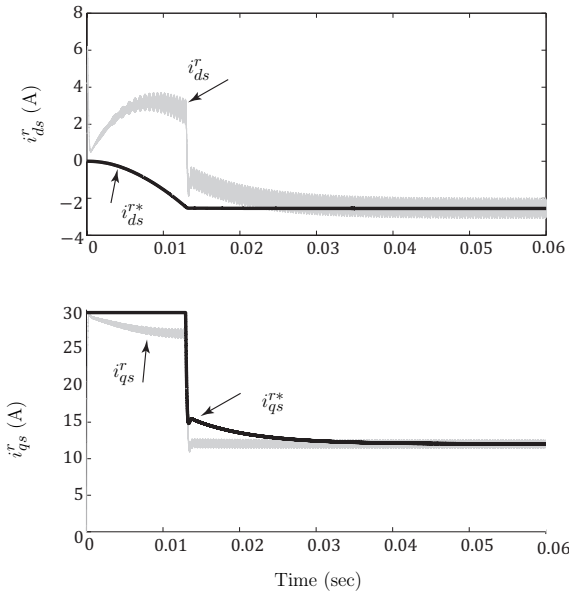


Fig. 5. Dynamic response of phase currents,  $i_{ds}^r$  and  $i_{qs}^r$  of surface mounted PMSM.

response in approximate 0.14 second for the system parameters listed in Table II. The current and speed controllers are designed by a symmetric optimum approach which is addressed in [4]. For calculation of the core loss resistance, it is required that the motor runs at rated speed and torque of sinusoidal power supply such that the harmonic losses are not generated. The fundamental iron loss  $P_{Fe}$  is calculated by subtracting the mechanical and copper losses from the total output power. The iron loss resistance,  $R_c$ , can be obtained from fundamental core losses as in (18), where the measured  $R_c$  represents the iron loss resistance at the rated output power. Practically  $R_c$  depends on operating conditions. However, it is assumed constant in this work.

Fig. 7 shows the efficiency of surface mounted PMSM versus speed for the two control strategies: zero  $i_d$  control strategy and (LMC) strategy. It is clear that the motor efficiency under maximum efficiency control strategy is higher than the efficiency under zero  $i_d$  control strategy. However, the difference in efficiency is not as remarkable for surface mounted PMSM as for interior PMSM due to the following reasons. In interior PMSM The negative d-axis current produces a positive reluctance torque due to the saliency ( $L_d < L_q$ ), and accordingly the stator current and the copper loss  $P_{Cu}$  is smaller compared with the  $i_d = 0$  control. Moreover, in both types of PMSMs the negative d-axis current reduces the flux linkage. Consequently, the voltage  $V$ , and the iron loss  $P_{Fe}$ , are smaller as compared with the  $i_d = 0$  control strategy [4]. Since the surface mounted PMSM has no saliency ( $L_d = L_q$ ), there is no reluctance torque. However, the influence of the decreased flux linkage and applied voltage is still effective.

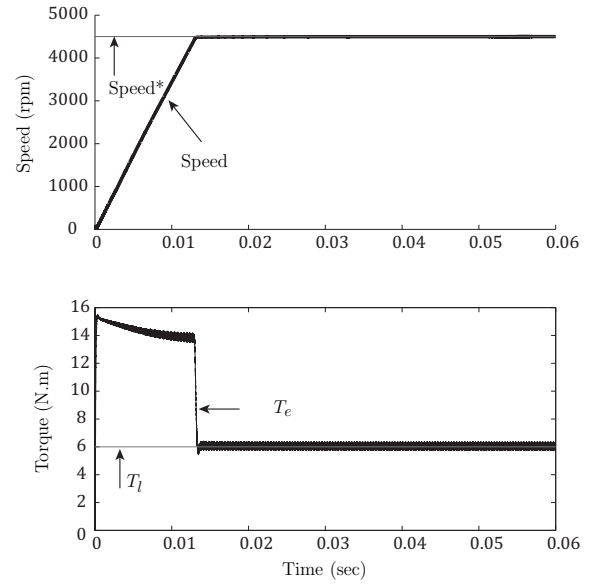


Fig. 6. Torque and speed dynamic response of surface mounted PMSM.

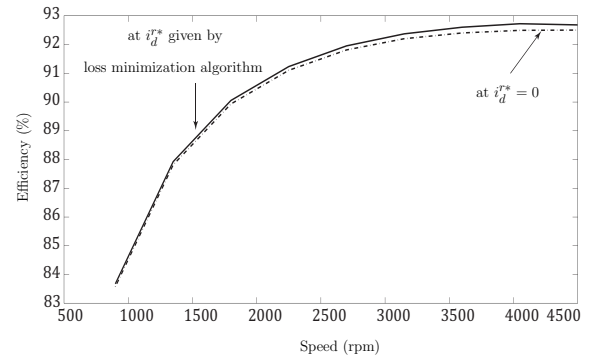


Fig. 7. PMSM efficiency versus speed.

### B. VSI and PMSM Fundamental Losses

As presented in Section III, the losses of VSI are divided into conduction losses and switching losses. Since the switching loss is proportional to switching frequency and motor phase current, the switching loss increases/decreases for any increases/decreases in load torque or/and reference speed. In addition, the conduction loss is proportional to motor phase current, modulation index and the displacement factor. The modulation index is controlled by load and speed since any increase in load or speed requires higher current which is supplied via higher voltage. Therefore the modulation index increases as well to supply the required voltage. Regarding the displacement angle, its effect on conduction loss is discussed in Section III.

Fig. 8(a) illustrates the relationship between motor fundamental loss and  $i_d^r$  under loss minimization control strategy. The curve is convex with global minimum loss point at  $i_d^r = -2.6$  A for the given parameter in Table II. Fig. 8(b) shows the relationship between the inverter losses and  $i_d^r$ . The result shows that the minimum loss point occurs at  $i_d^r = 0$

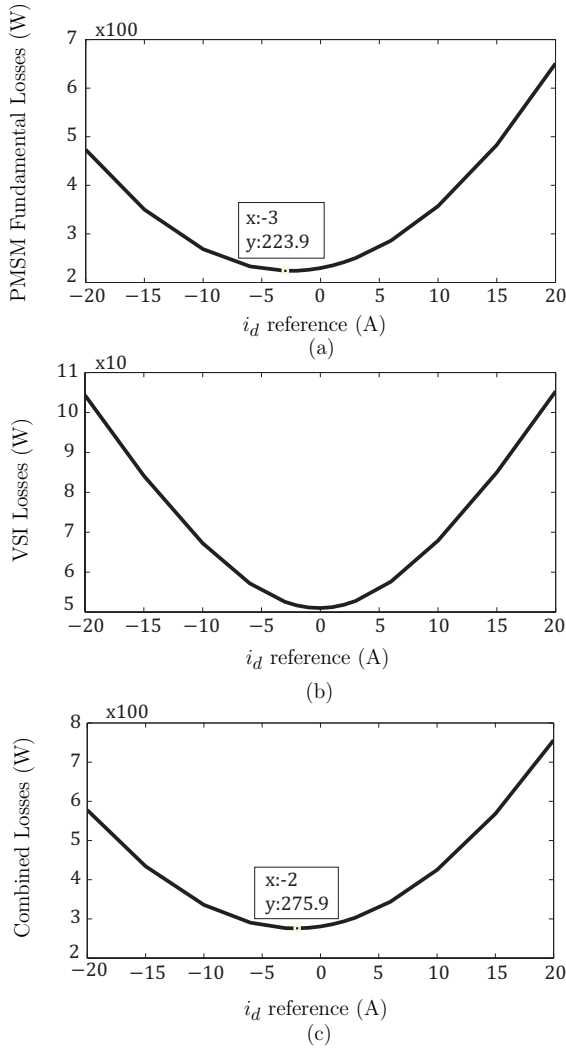


Fig. 8. Motor-inverter fundamental losses versus  $i_d^{r*}$  at rated speed: (a) PMSM fundamental losses; (b) VSI losses; (c) Combined fundamental losses of PMSM and VSI.

. This result can be explained as following: the rms value of the phase current is  $\sqrt{i_d^2 + i_q^2}$ . When  $i_d = 0$ , it is clear that the phase current has the minimum value. However, it was explained that most inverter loss is controlled by the current. When the phase current is minimum the inverter loss will be minimum as well. Fig. 8(c) shows the relationship between the combined losses of motor and inverter versus  $i_d^r$ . The relationship shows that the combined minimum loss value of inverter and motor occurs at a point of  $i_d^r$  that lies between the zero  $i_d^r$  and the optimal  $i_d^r$  that is generated by loss minimization algorithm.

For all conditions of loads and speeds, it can be observed that the inverter minimum loss value occurs at zero  $i_d^r$ , and the  $i_d^r$  generated by loss minimization algorithm is always negative for the same conditions. Moreover, the combined minimum loss value will strictly lie in the region between zero  $i_d^r$  and  $i_d^r$  generated by minimum loss algorithm.

### C. VSI and PMSM harmonic losses

The motor harmonic losses at any operating point can be calculated as the following. First The machine operates at rated speed and torque off sinusoidal power supply. The input power is then measured and the copper losses and output power are calculated, which gives motor efficiency and fundamental core losses. The same procedure is repeated except that the motor is supplied with SPWM-variable speed drive controller under the same torque and speed conditions. The core losses that are calculated with SPWM represent the summation of fundamental and harmonic losses at rated output power. Subtracting the sinusoidal-core losses from SPWM-core losses yields the motor harmonics loss at rated torque and speed. At  $T_e = 6 \text{ N} \cdot \text{m}$  and  $N = 4500 \text{ rpm}$  the calculated harmonics loss is  $90.8445 \text{ W}$ . However, the motor efficiency is reduced from  $92.68$  to  $90 \%$  when switching the sinusoidal supply with SPWM-variable speed drive controller. In PMSM the hysteresis losses are very small and can be neglected. In this work the hysteresis losses value is assumed to be  $5\%$  of the total harmonic losses.

$$P_{e,h} = 0.95P_{c,h}; \quad P_{h,h} = 0.05P_{c,h} \quad (20)$$

The next step is to calculate the coefficients  $K_{em}$  and  $K_{hm}$  :

$$K_{em} = \frac{P_{e,h}}{\sum_{m=1}^{\infty} \sum_{n=-\infty}^{\infty} (\omega_{m,n} |I_{m,n}|_{\omega \neq \omega_o})^2} \quad (21)$$

$$K_{hm} = \frac{P_{h,h}}{\sum_{m=1}^{\infty} \sum_{n=-\infty}^{\infty} (\omega_{m,n} |I_{m,n}|_{\omega \neq \omega_o})^2}$$

The calculated values are  $K_{em} = 3.8729 \times 10^{-8}$  and  $K_{hm} = 0.0013$ . The harmonic losses in [W] for any operating condition is:

$$P_{c,h} = 3.8729 \times 10^{-8} \sum_{m=1}^{\infty} \sum_{n=-\infty}^{\infty} (\omega_{m,n} |I_{m,n}|_{\omega \neq \omega_o})^2 + 0.0013 \sum_{m=1}^{\infty} \sum_{n=-\infty}^{\infty} \omega_{m,n} (|I_{m,n}|_{\omega \neq \omega_o})^2 \quad (22)$$

The motor harmonics loss, VSI loss and the total loss versus switching frequency are shown in Fig. 9. The results show that the PMSM harmonics loss decreases as the switching frequency increases. Nevertheless, the VSI losses increase as the switching frequency increase. The summation of the above two losses show that the curve is convex and has global minimum loss value at the switching frequency of  $19 \text{ kHz}$ . However the specific optimal switching frequency will depend on particular set of design parameters of the VSI. In other words, when the parameters of the VSI such that the loss of VSI higher than the motor harmonics loss at the same range of switching frequency, the curve will be no more convex and almost will be linear.

Fig. 10 shows the relationship between PMSM harmonic loss and modulation index. It can be seen that up to  $M = 0.73$



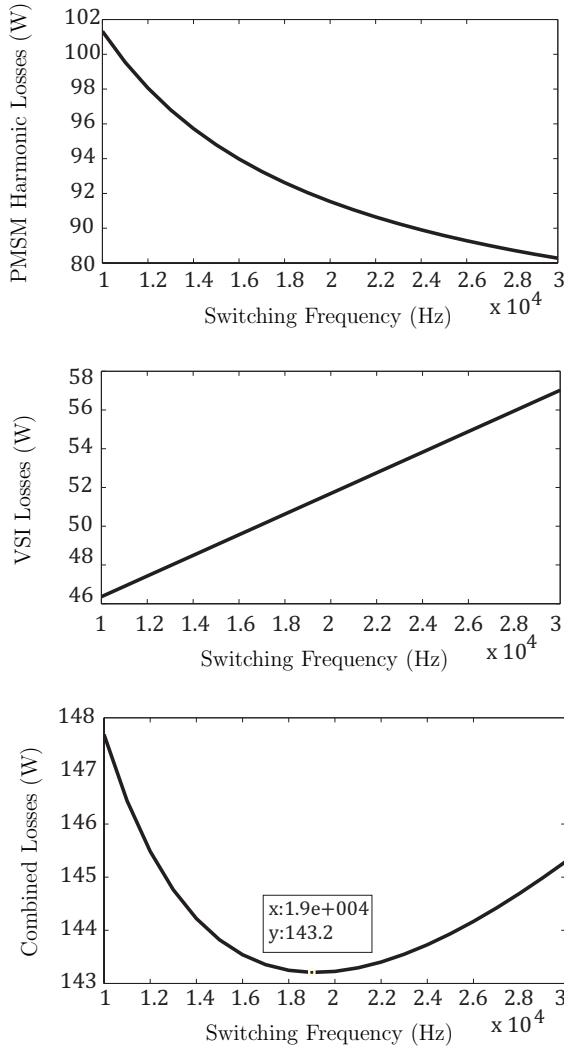


Fig. 9. Harmonic losses of PMSM, VSI losses and the combined harmonic losses of PMSM and VSI versus switching frequency at rated speed.

the harmonics loss increases as the modulation index increases. As the modulation index passes  $M = 0.73$ , the harmonics loss begins to decrease to locally minimum loss value at unity modulation index. Because the loss is minimum near unity modulation index, it is suitable to use variable dc link such that the modulation index is kept near the unity at all operating conditions.

## VI. CONCLUSIONS

The main results of the work can be summarized in the following aspects:

- The motor loss that is caused by the fundamental component of phase currents can be minimized by using the maximum efficiency control strategy with the assumption that the core loss resistance and copper loss resistance are constant under all operating conditions.
- The combined motor-inverter fundamental losses are minimized under maximum efficiency control strategy in the region in which  $i_d^{r*} < i_d < 0$ .

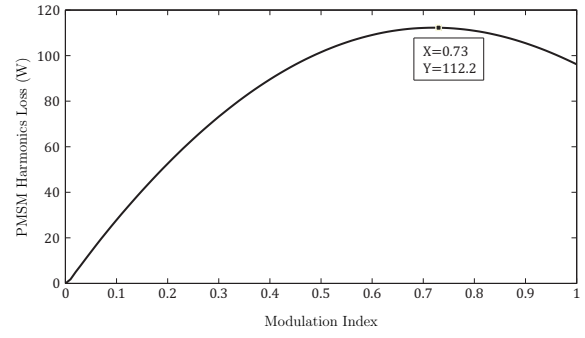


Fig. 10. PMSM harmonics loss versus modulation index.

- PMSM harmonics loss can be minimized by increasing the converter switching frequency with the assumption that SPWM inverter is used without any harmonics injection technique.
- For a given range of switching frequencies in which the motor can work with acceptable performance, the choice of minimal switching frequency would minimize the converter loss.
- For a given range of switching frequencies in which the motor can deliver acceptable performance, the choice of the optimum switching frequency that will minimize motor-inverter losses follows the parametric optimization. The optimal loss point is affected by the system parameters. Hence, changing of the values of VSI parameters would vary the optimal point of motor-inverter losses.

## REFERENCES

- [1] D. S. Kirschen, D. W. Novotny, and T. A. Lipo, "On-line efficiency optimization of a variable frequency induction motor drive," *Industry Applications, IEEE Transactions on*, vol. IA-21, no. 3, pp. 610–616, 1985.
- [2] R. Colby and D. Novotny, "Efficient operation of pm synchronous motors," *IEEE Transactions on Industry Applications*, vol. IA-23, no. 6, pp. 1048–1054, Nov./Dec. 1987.
- [3] L. Xu, X. Xu, T. Lipo, and D. Novotny, "Vector control of a synchronous reluctance motor including saturation and iron loss," *IEEE Transactions on Industry Applications*, vol. 27, no. 5, pp. 978–985, Sep./Oct. 1991.
- [4] S. Morimoto, Y. Tong, Y. Takeda, and T. Hirasa, "Loss minimization control of permanent magnet synchronous motor drives," *IEEE TRAN. on Industrial Electronics*, vol. 41, no. 5, pp. 511–517, Oct 1994.
- [5] G. Slemon and X. Liu, "Core losses in permanent magnet motors," *IEEE Transactions on Magnetics*, vol. 26, no. 5, pp. 1653–1655, sep 1990.
- [6] R. Schifer and T. Lipo, "Core loss in buried magnet permanent magnet synchronous motors," *Energy Conversion, IEEE Transactions on*, vol. 4, no. 2, pp. 279–284, jun 1989.
- [7] M. Bierhoff and F. Fuchs, "Semiconductor losses in voltage source and current source igbt converters based on analytical derivation," ser. in Proc. Power Electronics Specialists conference, vol. 4, 2004, pp. 2836–2842.
- [8] C. Mi, G. R. Slemon, and R. Bonert, "Modeling of iron losses of permanent-magnet synchronous motors," *IEEE Trans. Ind. Appl.*, vol. 39, no. 3, pp. 734–742, May 2003.
- [9] Z. Zhu and D. Howe, "Instantaneous magnetic field distribution in brushless permanent magnet dc motors. ii. armature-reaction field," *IEEE Transactions on Magnetics*, vol. 29, no. 1, pp. 136–142, Jan. 1993.
- [10] D. G. Holmes and T. A. Lipo, *Pulse Width Modulation for Power Converters*. John Wiley & Sons, 2003.